

Demand response for residential building heating: Effective Monte Carlo Tree Search control based on physics-informed neural networks

Fabio Pavirani^a, Gargya Gokhale^a, Bert Claessens^{a,b} and Chris Develder^a

^a*IDLab Ghent university – imec, Technologiepark Zwijnaarde 126, 9052 Gent, Belgium*

^b*Beebop, Belgium*

ARTICLE INFO

Keywords:

Building Control
Demand Response
Monte Carlo Tree Search
Physics informed Neural Network
Machine Learning
Thermal dynamics modeling

ABSTRACT

Controlling energy consumption in buildings through demand response (DR) has become increasingly important to reduce global carbon emissions and limit climate change. In this paper, we specifically focus on controlling the heating system of a residential building to optimize its energy consumption while respecting user's thermal comfort. Recent works in this area have mainly focused on either model-based control, e.g., model predictive control (MPC), or model-free reinforcement learning (RL) to implement practical DR algorithms. A specific RL method that recently has achieved impressive success in domains such as board games (go, chess) is Monte Carlo Tree Search (MCTS). Yet, for building control it has remained largely unexplored. Thus, we study MCTS specifically for building demand response. Its natural structure allows a flexible optimization that implicitly integrate exogenous constraints (as opposed, for example, to conventional RL solutions), making MCTS a promising candidate for DR control problems. We demonstrate how to improve MCTS control performance by incorporating a Physics-informed Neural Network (PiNN) model for its underlying thermal state prediction, as opposed to traditional purely data-driven Black-Box approaches. Our MCTS implementation aligned with a PiNN model is able to obtain a 3% increment of the obtained reward compared to a rule-based controller; leading to a 10% cost reduction and 35% reduction on temperature difference with the desired one when applied to an artificial price profile. We further implemented a Deep Learning layer into the Monte Carlo Tree Search technique using a neural network that leads the tree search through more optimal nodes. We then compared this addition with its Vanilla version, showing the improvement in computational cost required.


1. Introduction

Even though recently the energy sector already underwent a rather drastic transformation (e.g., via the increased penetration of renewable energy sources, RES), given the urgent need to combat climate changes, it is pressed even further to optimize energy consumption and reduce carbon emission. The rising contribution of RES leads to higher uncertainty, calling for Demand Response (DR) control to stabilize the grid. On top of that, a substantial part of energy consumption stems from the residential sector: in the EU, it represented 26.1% of the total energy in 2018 [1]. Of that residential energy, 63.6% is used for heating [1]. This high portion of energy consumed in the residential heating domain, combined with the uncertainty given by RES, implies a great potential for flexible and effective controllers that can manage varying constraints.

To realize sequential residential heating control, two main strategies have been followed [2]: either (i) model-based controllers, or (ii) purely data-driven controllers. For (i), typically Model Predictive Control (MPC) is adopted, where a model of the building's thermal dynamics is integrated into an optimization problem. This optimization problem is solved to obtain or approximate an optimal control decision. Model-based techniques, although very efficient, are highly dependent on the model used and can

be difficult to scale over different houses [3]. On the other hand, regarding purely data-driven controllers, one of the most used techniques is Reinforcement Learning RL, which is more flexible and scalable towards different households. However, it requires a large amount of data obtained by interacting with the building [4], which is usually hard to obtain. A solution to this problem is to develop a simulator for the RL agent to interact with, adding once again more importance to the modeling task. Despite their promising results in producing effective control policies, several challenges regarding RL algorithms in the Building Energy Management (BEM) domain are yet to be solved, such as their lack of interpretability and safety [4], as well as their flexibility when dealing with exogenous constraints, e.g., user temperature bounds or grid balancing signals. To tackle these problems, inspired by recent Monte Carlo Tree Search (MCTS) algorithms such as MuZero [5], we present an RL framework for energy cost and thermal comfort optimization that is able to directly manage varying exogenous constraints while also producing flexible control actions.

To model the thermal dynamics of a building, we developed a Physics informed encoder-based Neural Network forecaster, expanding the PhysNet presented by Gokhale et al. [6] to a multi-step prediction model. Then, using the model as a simulator, we developed an MCTS algorithm that optimizes energy cost while following user-defined constraints. The main hypotheses that we will verify through this paper are the following:

 fabio.pavirani@ugent.be (F. Pavirani)

ORCID(s): 0009-0005-7904-099X (F. Pavirani); 0000-0002-1451-397X

(G. Gokhale); 0009-0006-6116-1483 (B. Claessens); 0000-0003-2707-4176

(C. Develder)

- H1:** Our extension to the PhysNet architecture (Section 3.2) improves forecasting performance compared to purely data-driven models when used in multi-step forecasting problems of a residential household thermal dynamics (Section 5.1);
- H2:** Our Physics-informed Neural Networks model can substantially improve the control performance of an MCTS algorithm compared to Black-Box models (Section 5.2);
- H3:** Adding a Deep Learning (DL) layer to MCTS techniques to guide the tree search (Section 3.3) can optimize the computational effort required when applied to the BEM residential domain (Section 5.3).

2. Literature review

Below we summarize previous work relevant to this paper, focusing in particular on thermal modeling and Demand Response control of buildings.

2.1. Thermal dynamics modeling of buildings

Creating an accurate and scalable model that describes the thermal dynamics of a building is crucial to obtain a sequential controller. These models can be divided into three main categories: white-box models, Black-Box models and hybrid models [7–14]. White-box models (or first principle models) are typically physics-based methods that model the system using Ordinary Differential Equations [15, 16]. Despite their accuracy, the main drawback of white-box models is the complexity of the physical model developed [8] that obstructs scalability. Conversely, Black-Box methods try to model the thermal dynamics of a building by learning from historical data. Yet, Black-Box models such as Artificial Neural Networks (ANN) suffer from generalization issues [17] and hence need a large and complete dataset, which often is hard to obtain [18].

2.1.1. Hybrid models

Hybrid models (or gray-box models) combine both Black-Box and white-box models, trying to solve their respective limitations while exploiting their good features. The idea is to use generic and usually manageable physical equations together with data-based training to obtain a simple yet accurate model of the building [8, 19, 20]. Because of their simplicity, linear RC models are often used for this [21, 22].

2.1.2. Physics-informed neural networks

One particular subfamily of hybrid models is based on Physics-informed Neural Networks (PiNN) [23], where an ANN that incorporates physical prior knowledge into the prediction process is used. The idea of adapting the Neural Network (NN) structure and its training process to a specific kind of problem is not new in the DL literature. The most successful architectures that are used for this include Long Short-Term Memory modules [24], Convolutional Neural Networks [25] and Triplet Neural Network loss [26]. For

modeling the thermal dynamics of buildings, different types of PiNNs have already been applied [6, 18, 27]. Gokhale et al. [6] modified the loss function of an encoder-based NN to guide it toward physical adherence of the latent state. Drgoña et al. [27] modeled the state, input, disturbance, and output matrices of a classical linear equation using four different NNs and enforced physical constraints on them. Di Natale et al. [18] modeled the NN architecture to enforce physical consistency on its prediction.

This subfamily of models is particularly relevant for the problem of optimal control action search thanks to their ability to provide accurate non-linear system correlations related to the well-studied ANN methods, while also providing some level of physical consistency through the model predictions. Last, PiNN has shown promising results regarding their sample efficiency, requiring less data for acceptable results compared to purely Black-Box models [6]. All of these features are crucial when training an agent for building demand response control.

2.2. Demand response control of buildings

In the last decades, an increasing amount of work has focused on Demand Response [2]. With this term we refer to the problem of obtaining control policies that react to external signals (e.g., a cost profile, the desired temperature). These control algorithms can be roughly classified into two main categories: Model Predictive Control (MPC) and Reinforcement Learning (RL) approaches.

2.2.1. Model Predictive Control

With MPC, an optimization problem is solved (or approximated) for each control action in a receding horizon approach. This kind of technique is model-biased and requires an accurate model to get satisfactory results. As outlined in Section 2.1, models can be either White-box, Black-box, or Gray-box, each with their respective benefits and drawbacks. All three approaches have been applied successfully in real applications [28]. A more detailed list and review of different MPC techniques can be found in [29]. Although White-box MPC models have been shown to be promising, their application needs a non-negligible amount of expert knowledge about the problem configuration, making it difficult to generalize to different situations. For this reason, data-driven MPC algorithms have received increasing attention. Among these, Deep Learning MPC methods are the most popular [30–33]. Compared to linear models that can be readily solved using commercial solvers [34], non-linear models like ANN may be more complicated to use in optimization problems, adding complexity to ANN-based MPC algorithms and limiting their application.

2.2.2. Reinforcement Learning

Another family of data-driven algorithms that showed promising results in the last decade is Reinforcement Learning. RL algorithms formalize the system to control as a Markovian Decision Process (MDP) and interact with it to learn an adequate policy that tries to maximize the expected reward obtained from the environment. Such RL controllers

have been applied successfully to several problems in the BEM domain [35–39]. However, multiple challenges arise with RL techniques. For example, RL algorithms usually require a large amount of data for training to reach acceptable performance. Also, most RL algorithms used in the BEM environment are model-free [3], which often obstructs an effective planning approach that considers dynamic constraints.

2.2.3. Monte Carlo Tree Search

Monte Carlo Tree Search (MCTS) can be a solution to the problems described above. MCTS has already been applied as a DR planning method for balancing the electrical grid [40–43]. For residential DR with a heating system, Kiljander et al. [44] used MCTS, modeling the thermal dynamic of a household using a Feed Forward Neural Network (FFNN), and using it as a simulator with a standard MCTS algorithm to obtain planning decisions evaluated in a real house. We follow a similar approach by considering a PiNN architecture to model the household and adding a DL layer to an MCTS algorithm inspired by the recent success of Silver et al. [45, 46]. Using an MCTS-based controller enables to implicitly manage future exogenous constraints by trimming off actions that would lead to violating them. Also, by using hybrid models as a simulator instead of a Black-Box one, more reliable results are obtained while retaining the scalability of Black-Box models.

In this paper, we want to evaluate MCTS control ability in a residential heater DR problem. MCTS's structure enables a planning framework that can simplify constraints management, making the algorithm a promising candidate for DR applications. The solution methodology is described in Section 3.3.

3. Mathematical formulation

3.1. Markov Decision Process

We model the sequential control problem of heating a household as a Markov Decision Process (MDP) [47]. An MDP is a mathematical structure described by the tuple (X, U, f, ρ) where X is the state space, U is the action space, $f : X \times U \times X \rightarrow [0, 1]$ is the state transition probability function and $\rho : X \times U \times X \rightarrow \mathbb{R}$ is the reward function. Through this mathematical structure, we can model the control problem as an optimization problem to find the control policy $\pi : X \rightarrow U$ that maximizes the expected reward obtained from the environment. Formally, given a policy π , we consider the definition of its Q-function [47]:

$$Q^\pi(x, u) \doteq \mathbb{E}_{x' \sim f(x, u, \cdot)} [\rho(x, u, x') + \gamma R^\pi(x')],$$

where:

$$R^\pi(x_0) \doteq \lim_{T \rightarrow +\infty} \mathbb{E}_{x_{t+1} \sim f(x_t, \pi(x_t), \cdot)} \left[\sum_{t=0}^T \gamma^t \rho(x_t, \pi(x_t), x_{t+1}) \right].$$

We then consider the definition of the optimal Q-function [47], that is:

$$Q^*(x, u) \doteq \max_{\pi} Q^\pi(x, u).$$

The optimization problem is then to find an optimal policy π^* [47] such that:

$$\pi^*(x) \in \arg \max_u Q^*(x, u); \forall x \in X.$$

For simplicity of notation, in this work we consider the set W that contains the influence that adds stochasticity into the system dynamics. This set will be used in the next sections and will help have a more readable formulation of the problem.

MDPs can be classified into two distinct categories: Fully Observable Markov Decision Process (FOMDP) and Partially Observable Markov Decision Process (POMDP). With FOMDP, the states of the system $x \in X$ are fully observable by the policy π . Conversely, in POMDP only a subset of the state space $X^{\text{obs}} \subset X$ is observable by the policy: $\pi : X^{\text{obs}} \rightarrow U$.

To model the control problem of heating a household, we consider a stochastic POMDP to optimize the energy cost of the heating component while staying close to the desired temperature set by the users $T_{r,\text{set}}$. We use t to note the time-step index of each value. We define an observable state at a time-step t as: $x_t^{\text{obs}} = (T_{r,t}, u_{\text{phys},t-1}) \in X^{\text{obs}}$ where $T_{r,t}$ is the room temperature of the building we wish to control and $u_{\text{phys},t-1}$ is the energy consumed by the heating system in the $u_{\text{phys},t-1}$ previous time-step. The action $u \in U$ is a continuous single value indicating the control signal for the heating component. The exogenous influences are defined as $w_t = (\tau_t, T_{a,t}) \in W$ where $\tau_t \in [0, 24[$ indicates the hour of the day and $T_{a,t}$ is the outdoor temperature. The reward function is defined as:

$$\rho(x_t, u_t) \doteq \underbrace{-u_{\text{phys},t} \lambda_t}_{\text{Cost optimization}} - \underbrace{(T_{r,\text{set},t} - T_{r,t+1})^+ c_1 - (T_{r,t+1} - T_{r,\text{set},t})^+ c_2}_{\text{Thermal Comfort optimization}}, \quad (1)$$

where λ_t is the energy price at time-step t , $T_{r,\text{set},t}$ is the desired temperature set by the users and c_1, c_2 are hyperparameters used to balance the energy cost objective with the user constraints. The thermal comfort optimization uses an asymmetrical form ($c_1 > c_2$) to avoid excessive penalization for pre-heating the room. Last, the transition function f describes the thermal dynamics of the building. Because these dynamics are hard to fully describe mathematically, we approximate them by considering a deterministic FOMDP that resemble the POMDP described above by using a PiNN that represents the state transition function, as described in Section 4.1.

3.2. Physics-informed Neural Network

Considering a POMDP as described in Section 3.1, we use a PiNN architecture to forecast the next observable states of a system $x^{\text{obs}} \in X^{\text{obs}}$ by inserting physical equations into the learning loss function of the ANN. We follow the PhysNet structure proposed by Gokhale et al. [6] by deploying an encoder-based neural network. PhysNet is specifically built

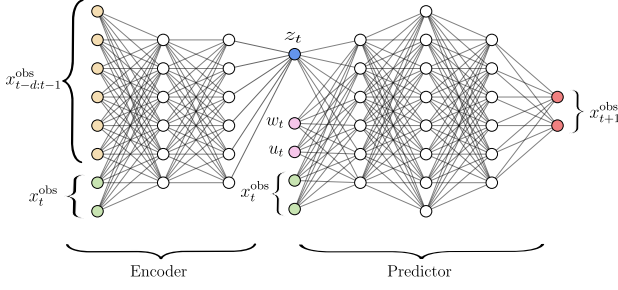


Figure 1: Architecture of the PiNN. Yellow nodes represent past observations, green nodes are the current observations, the pink nodes represent the current exogenous state and action, the blue node is the hidden state and the red nodes are the next predicted observations

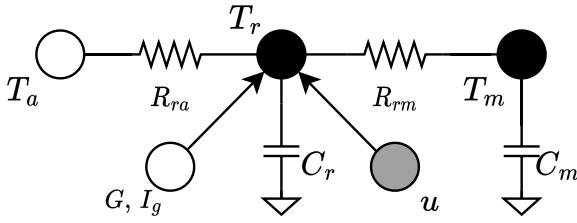


Figure 2: RC model used in the encoder loss [22].

for projecting a time-series of $d \in \mathbb{N}$ historical observable states $x_{t-d:t}^{obs} \doteq (x_{t-d}^{obs}, \dots, x_t^{obs})$ into a compact hidden state z_t , while training the ANN such that these latent values adhere to certain physical values. The obtained hidden state z_t , together with the current observable state x_t^{obs} , the current action $u_t \in U$ and the exogenous state $w_t \in W$ are processed by a separate predictor component that will return the next observable state x_{t+1}^{obs} prediction. The overall structure of the architecture is captured in Fig. 1.

We expanded the model [6] to obtain a multi time-step forecast by deploying a sequential, autoregressive, multi-loss training loop with windowed inference. We considered the 2R2C model [22] shown in Fig. 2 to infuse physical knowledge into the encoder training. The physical equations obtained are then:

$$\begin{bmatrix} \dot{T}_r \\ \dot{T}_m \end{bmatrix} = \begin{bmatrix} -\left(\frac{1}{C_r R_{ra}} + \frac{1}{C_r R_{rm}}\right) & \frac{1}{C_r R_{rm}} \\ \frac{1}{C_m R_{rm}} & -\frac{1}{C_m R_{rm}} \end{bmatrix} \cdot \begin{bmatrix} T_r \\ T_m \end{bmatrix} + \begin{bmatrix} \frac{c_p T_s}{C_r} \\ 0 \end{bmatrix} \cdot \dot{u} + \begin{bmatrix} \frac{1}{C_r R_{ra}} & \frac{\gamma}{C_r} & \frac{1}{C_r} \\ 0 & 0 & 0 \end{bmatrix} \cdot \begin{bmatrix} T_a \\ G \\ I_g \end{bmatrix}. \quad (2)$$

Here, T_m indicates the building mass temperature. The rest of the symbols follow the notation used in Vrettos et al. [22]. The NN structure is designed to predict the next observable state for each prediction. The output of the predictor is then used as input for the next predictions in an autoregressive loop to extend the prediction horizon up to a desired number

of time-steps $h \in \mathbb{N}^+$. To further incentivize the model's generalization ability, the predictor is trained to forecast the room temperature difference between the current observable state and the next one. To train the PhysNet, two different losses are integrated into the training loop: one regression loss responsible for the observable states prediction, and one physics loss responsible for the adherence of the latent space with the thermal mass physical values:

$$\mathcal{L} = \mathcal{L}_{\text{reg}} + \mathcal{L}_{\text{phys}}.$$

The regression loss is an L2 loss between the predicted observable states and the measured ones:

$$\mathcal{L}_{\text{reg}} \doteq \sum_{t=1}^N (\hat{x}_{t+1:t+h}^{\text{obs}} - x_{t+1:t+h}^{\text{obs}})^2.$$

The physics loss is used to train the hidden state prediction. It consists of another L2 loss that compares the predicted mass temperatures vector with a target vector $\hat{\mathbf{T}}_m^t$. To better understand the training process of the encoder, we introduce the following notations:

- We define $\mathbf{T}_m^t \in \mathbb{R}^h$ as the vector containing the h autoregressive predictions of the mass temperatures (i.e., of the hidden states) when starting the prediction from the time-step t ;
- We define $\mathbf{T}_r^t \in \mathbb{R}^h$ as the vector containing the h measured room temperatures starting from the time-step t .

The target value for the encoder training when starting from the time-step t is then defined by applying Eq. (2) as:

$$\hat{\mathbf{T}}_m^t = \mathbf{T}_m^{t-1} + \frac{\Delta_t}{C_m R_{rm}} (\mathbf{T}_r^{t-1} - \mathbf{T}_m^{t-1}), \quad (3)$$

where Δ_t is the duration of a time-step. The loss function to be minimized for the predictions starting from time-step t will then be:

$$\mathcal{L}_{\text{phys}} \doteq \sum_{t=1}^N (\hat{\mathbf{T}}_m^t - \mathbf{T}_m^t)^2.$$

To study the impact of the PiNN component, we also perform a Black-Box ablation that omits $\mathcal{L}_{\text{phys}}$. More details about the neural networks hyperparameters are in Appendix A.

3.3. Monte Carlo Tree Search

MCTS models the states of the environment as nodes and the actions as edges in a tree representing the possible scenarios that the current state may evolve into. We will consider deterministic environments with the assumption that a generative model of the MDP is available (i.e., the environment is simulable). To differentiate these deterministic and simulable MDPs from the stochastic ones introduced in Section 3.1, we will adopt the following notation: we will refer to the state space of the environment as \bar{X} , the

action space as \tilde{U} , the transition function as $\tilde{f} : \tilde{X} \times \tilde{U} \rightarrow \tilde{X}$ and the reward function as $\tilde{r} : \tilde{X} \times \tilde{U} \rightarrow \mathbb{R}$. MCTS was first introduced in 2006 by Coulom [48] and gain its popularity thanks to UCT [49]. The general structure of the algorithm can be described in four sequential phases that are repeated iteratively:

- i **Selection:** select an edge in the tree until a leaf node is reached.
- ii **Expansion:** expand the tree by adding new node(s).
- iii **Simulation:** evaluate the node value by performing Monte Carlo simulations.
- iv **Backpropagation:** propagate the information acquired back to the root node.

These phases are repeated multiple times. At the end of the search, the best action is selected based on the optimal value approximation obtained. For selection's equations like UCT, it has been proven that this search converges to the optimal solution [49]. New implementations have been made in the last decades by, for example, changing the UCT score formula [50] and adding NNs for value and policy estimation in the tree search [5, 45, 46, 51].

In our experiments, we make use of some of the most recent improvement made to MCTS, strongly inspired by the work of [5, 46]. The algorithm consists of a sequence of three phases repeated iteratively:

1. **Selection:** Starting from a root node $\tilde{x}^0 \in \tilde{X}$, the tree is traversed by selecting the action $\tilde{u}^k \in \tilde{U}^k$; $k \in \mathbb{N}$ until a leaf node \tilde{x}^l is reached. We use a dynamic action space $\tilde{U}^k \subseteq \tilde{U}$; $\forall k \in \mathbb{N}$ that represents the allowed actions from state \tilde{x}^k with respect to the environment-based constraints. The selection of each action in this phase is based on:

$$\tilde{u}^k = \arg \max_{\tilde{u} \in \tilde{U}^k} \left\{ \underbrace{\tilde{Q}(\tilde{x}^k, \tilde{u})}_{\text{Value score}} + \alpha \underbrace{\frac{\sqrt{N(\tilde{x}^k)}}{1 + N(\tilde{x}^k, \tilde{u})}}_{\text{Exploration score}} \right\}; \quad (4)$$

$\forall k \in 0, 1, \dots, l-1$

where $N(\tilde{x})$ is the number of time the node \tilde{x} has been reached following an action selected in Eq. (4), $N(\tilde{x}, \tilde{u})$ is the number of times the action \tilde{u} has been selected in Eq. (4) from state \tilde{x} , $\tilde{Q}(\tilde{x}, \tilde{u})$ is a state-action value function that estimates the expected future average rewards obtained by executing the action \tilde{u} from state \tilde{x} . α is a hyperparameter used to balance the exploration-exploitation trade-off. In our experiments, we set $\alpha = 1$, unless stated otherwise.

2. **Expansion:** Once a leaf node \tilde{x}^l is reached, if its depth does not exceed a fixed maximum value, the leaf gets expanded by adding new nodes, one for each possible action: $\tilde{U}^l \subseteq \tilde{U}$.

3. **Backpropagation:** After the expansion phase, statistical information about the reward obtained in the selected trajectory gets backpropagated until the root node. In particular, starting from the leaf node, the \tilde{Q} function gets updated as:

$$\tilde{Q}(\tilde{x}^k, \tilde{u}^k) = \frac{N(\tilde{x}^k, \tilde{u}^k)\tilde{Q}(\tilde{x}^k, \tilde{u}^k) + \frac{G^{k+1}}{(l-k)}}{N(\tilde{x}^k, \tilde{u}^k) + 1}; \quad (5)$$

$\forall k = l-1, \dots, 0$

where $\tilde{Q}(\tilde{x}^k, \tilde{u}^k)$ is initialized as $\tilde{r}(\tilde{x}^k, \tilde{u}^k)$ and G^k is the discounted accumulated reward defined as:

$$\begin{cases} G^l = \tilde{r}(\tilde{x}^{l-1}, \tilde{u}^{l-1}) \\ G^k = \tilde{r}(\tilde{x}^{k-1}, \tilde{u}^{k-1}) + \gamma G^{k+1}; \forall k = l-1, \dots, 1 \end{cases} \quad (6)$$

where γ is the discount value.

It is important to note that $\tilde{Q}(\tilde{x}, \tilde{u})$ is not intended as the expected cumulative reward of performing action \tilde{u} from state \tilde{x} (i.e., the interpretation of a Q function in classical RL). In fact, \tilde{Q} is the approximation of the expected average reward, conversely to the classical RL interpretation of a Q function that makes use of the Bellman equations.

The rewards $\tilde{r}(\tilde{x}, \tilde{u})$ considered in this algorithm are normalized between 0 and 1, ensuring that every \tilde{Q} value in Eq. (5) is also contained in $[0, 1]$. At the end of these repeated phases, the optimal action is obtained by considering the most selected edge of the tree during the Selection phase (Eq. (4)). We will refer to this algorithm as Vanilla MCTS. To further evaluate MCTS techniques in the BEM domain, we also deployed a more advanced version that uses a NN to lead the tree search through more optimal nodes, similarly to what was proposed in [46]. The algorithm follows the same structure as described above and changes Eq. (4) to:

$$\tilde{u}^k = \arg \max_{\tilde{u} \in \tilde{U}^k} \left\{ \underbrace{\tilde{Q}(\tilde{x}^k, \tilde{u})}_{\text{Value score}} + P(\tilde{x}^k, \tilde{u}) \alpha \underbrace{\frac{\sqrt{N(\tilde{x}^k)}}{1 + N(\tilde{x}^k, \tilde{u}^k)}}_{\text{Exploration score}} \right\}; \quad (7)$$

$\forall k \in 0, 1, \dots, l-1$

Where $P(\tilde{x}, \tilde{u})$ is a prior probability value associated to action \tilde{u} from state \tilde{x} and approximated by a neural network $p(\tilde{x})$. The neural network is trained offline by using sampled trajectories obtained with the Vanilla MCTS algorithm, considering the FOMDP simulator for both the search and evaluation environment. We will refer to this algorithm as AlphaZero MCTS, following the name of the original work that inspired us [46]. When using AlphaZero MCTS, we fixed $\alpha = 3.5$. More details about the ANN structure are in Appendix A.

4. Application framework

4.1. Control-oriented modeling

We design a second MDP that will approximate the real household and will interact with the MCTS agent to gain optimal control actions. In particular: we design a FOMDP with deterministic dynamics described by the PhysNet introduced in Section 3.2, i.e., the exogenous information gets forecasted for a fixed horizon h to enable a deterministic simulation provided by the PiNN model. To differentiate it from the real household POMDP, we indicate this new environment with a different notation: $(\tilde{X}, \tilde{U}, \tilde{f}, \tilde{\rho})$, consistent with what we introduced in Section 3.3. The state at a certain time-step t is a continuous vector defined as:

$$\tilde{\mathbf{x}}_t \doteq (\tau_t, T_{r,t}, T_{m,t}) \in \tilde{X} \quad (8)$$

where: $\tau_t \in [0, 24]$ is the time of the day, $T_{r,t} \in \mathbb{R}$ is the room temperature and $T_{m,t} \in \mathbb{R}$ is the (predicted) mass temperature of the building. Because the PhysNet model requires a series of d past states to obtain the predicted mass temperature, we define an augmented state as:

$$\tilde{\mathbf{x}}_t^{\text{aug}} \doteq (T_{r,t-d:t-1}, u_{\text{phys},t-d-1:t-1}) \quad (9)$$

The action space is discrete and single-dimensional $\tilde{U} \subset U$, representing the heating system control action. The transition function \tilde{f} is a PiNN as described in Section 3.2. Last, the reward function $\tilde{\rho}$ is defined, similarly to the original one introduced in Eq. (1), as:

$$\tilde{\rho}(\tilde{x}_t, \tilde{u}_t) \doteq \underbrace{-u_{\text{phys},t} \lambda_t}_{\text{Cost optimization}} - \underbrace{(T_{r,\text{set},t} - T_{r,t+1})^+ c_1 - (T_{r,t+1} - T_{r,\text{set},t})^+ c_2}_{\text{Thermal Comfort optimization}} \quad (10)$$

This structure provides the capability to simulate future states — which approximate the real dynamics through using a PiNN — enabling the deployment of an MCTS algorithm.

4.2. Experiments set up

To train and evaluate our PiNN architecture, we used a benchmark model developed by Blum et al. [52]. We consider their single-zone Hydronic Heat Pump. In particular, we used BOPTTEST-Gym: an Open-AI-Gym implementation thereof developed by Arroyo et al. [53]. In this set-up, the action space consists of the modulation signal of the heat pump, that is: $U \doteq [0, 1]$.

To evaluate the Physnet forecasting ability, we used BOPTTEST-Gym to generate a time-series of data by simulating the heat pump usage with a continuous controller (details in Appendix B). The time-series data is being simulated starting by the first of January and is described in Table 1. We use a time-step length of 30 minutes. We add cumulative noise to the outside temperature to emulate the prediction error of a weather forecaster tool (see Appendix C for more details).

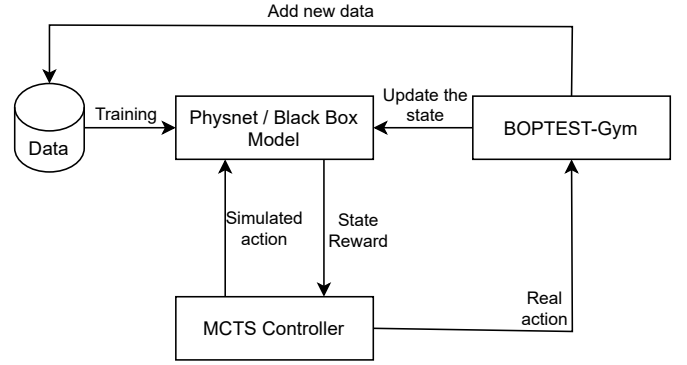


Figure 3: Controller structure. The simulator first gets trained with historical data. It is then used to build a tree search. The optimal action is then deployed in the real case, which updates the states of the simulator. These steps are repeated as needed.

Regarding the MCTS techniques evaluation, we first initialized the BOPTTEST-Gym Environment and simulated 10 days with a discrete rule-based controller (details in Appendix B). The data obtained by the simulations are then used to train the PhysNet (or the Black-Box) model. We then used our trained networks to build the tree search of the algorithms described in Section 3.3. When the tree search is completed, the best action is then applied to the BOPTTEST-Gym Environment, which provides the new state values to initialize another simulated environment. The process is then repeated as needed. The simulator's NNs are retrained after every day of evaluation by adding the newly obtained data into the training dataset. In our case, the algorithms are evaluated for a consecutive period of 11 days. The whole controller structure is illustrated in Fig. 3.

Because the MCTS algorithm works with discrete actions, we considered 5 equally spaced actions over the entire action space: $\tilde{U} \subset U \doteq [0, 1]$. To further analyze the MCTS algorithm's potential, we consider two different price situations: a realistic one with real-world price data; and a synthetic one, with an artificially built squared wave price data.

4.3. Constraints management

When using MCTS, we assume a backup controller that forces the heat pump to activate (respectively turn off) when the room temperature falls below the desired one by Δ_T^- (respectively exceeds it by Δ_T^+). The values and the relations described above are easily changeable based on the use case. In the MCTS framework, this backup controller translates to trimming the action edges, i.e., only keeping the actions as enforced by the Δ_T^\pm bounds. It is worth noting that such backup constraints can be picked with total freedom based on the available state values, so more complex constraints as opposed to just clipping could be integrated.

5. Results

In this section we aim to answer the following research questions:

Table 1
Description of the data used

Data name	Description	Value domain
τ	Hour of the day	[0, 24[
T_r	Indoor temperature [°C]	[15, 25]
T_a	Outside temperature measured in a dry bulb [°C]	[-10, 20]
u	Heat pump modulating signal for the compressor speed	[0, 1]
u_{phys}	Heat pump electrical power consumed [W]	[0, 4000]
λ	Belgian day-ahead energy prices as determined by the BELPEX electricity market [€/kWh]	[-0.4, 0.4]

- Q1:** Is the PhysNet model more *accurate and data-efficient* compared to a Black-Box model? (Section 5.1)
- Q2:** Is the PhysNet model able to provide *better control actions* when used in a Vanilla MCTS algorithm compared to a Black-Box model? (Section 5.2)
- Q3:** What computational benefits can we obtain by a more targeted tree search exploration (i.e., using AlphaZero MCTS instead of Vanilla MCTS)? (Section 5.3)

We present a sequence of three experiments that will answer these questions.

5.1. Forecasting results

We first compare the forecasting results of the PiNN model to its Black-Box counterpart to analyze the overall prediction metrics of both models and investigate their interpretability. We generated training sets of 2, 5, and 24 days using the BOPTTEST framework, with a prediction horizon of 3, 6, and 12 hours. Each trained model is then evaluated on a test set of 6 days. For each, we repeat the training process for 100 times to check the training stability. Using the Mean Absolute Error (MAE) of the predictions in the test set, Fig. 4 plots the median value and the interquartile range of the results.

We observe that the PhysNet model is more data efficient than the Black-Box model, confirming that infusing physical knowledge helps, for a small dataset, the temperature predictions. Yet, in terms of energy consumption prediction, the two models' performance is virtually the same. In both the temperature and energy consumption predictions, the results converge to the same values when provided with a large enough training dataset. Last, because the mass temperature of a building is difficult to measure, we cannot quantitatively evaluate the hidden state prediction of the PhysNet model with a numerical metric. Therefore, we empirically validate that the results follow an expected behavior. A plot of a whole prediction horizon of 12 hours in the test set is shown in Fig. 5. From a graphical analysis, we observe that the predicted T_m is varying with a higher delay compared to T_r , similarly to a physical value subject to a higher inertia. Even though we cannot validate the accuracy of such predictions, we can acknowledge that they follow an expected behavior, i.e., the mass temperature acts as a thermal storage that slowly releases (or absorbs) heat to (or from) the room.

5.2. PiNN control benefits

To further assess the PiNN model's benefits from a control perspective, we benchmark the cumulative reward obtained by the Vanilla MCTS algorithm when aligned with the PhysNet. We also considered a bang-bang rule-based controller as a baseline to further benchmark our results. Details of the bang-bang rule-based controller can be found in Appendix B. The reward is normalized between 0 and 1 for each time-step. We use different configurations of the MCTS algorithm's hyperparameters for each model, starting from a fast evaluation (low number of simulations and low tree depth) to a slower but more accurate evaluation (higher number of simulations and higher tree depth). The results are shown in Fig. 6. We clearly see that for both price profiles, a substantial improvement of the MCTS algorithm is achieved when using the PiNN model vs. the purely data-driven Black-Box one. We hypothesize that this is due to the higher physical consistency of the PiNN model when used in situations that are not seen in the training data, as previously observed by Di Natale et al. [18]. Last, in Fig. 7 we show two different policies applied to the same day. There we can observe how the MCTS controller is able to better follow to the desired temperatures (as observable, e.g., at time ~ 20 h), while using the heater at times with lower energy cost, leading to higher rewards compared to the rule-based controller.

5.3. DL-infused MCTS results

A drawback of the Vanilla MCTS algorithm is its slow execution time for each control action. As already shown for different problems [5, 46], the addition of prior knowledge into the tree search can increase its performance in terms of higher rewards at lower computational time. For this reason, we implemented the AlphaZero MCTS algorithm as described in Section 3.3. The NN used in Eq. (7) is trained offline at the end of each day by using simulated samples obtained with data from previous days. These samples are obtained by using the Vanilla MCTS algorithm and by searching and evaluating on the same simulated environment. Since training is performed offline, we choose a high enough number of tree traversals to sample our simulated trajectories. We then compared the results of the Vanilla MCTS algorithm with this AlphaZero MCTS algorithm. Figure 8 shows the daily average cumulative reward obtained using the PiNN model. The results show a noticeable improvement in the obtained rewards for the AlphaZero

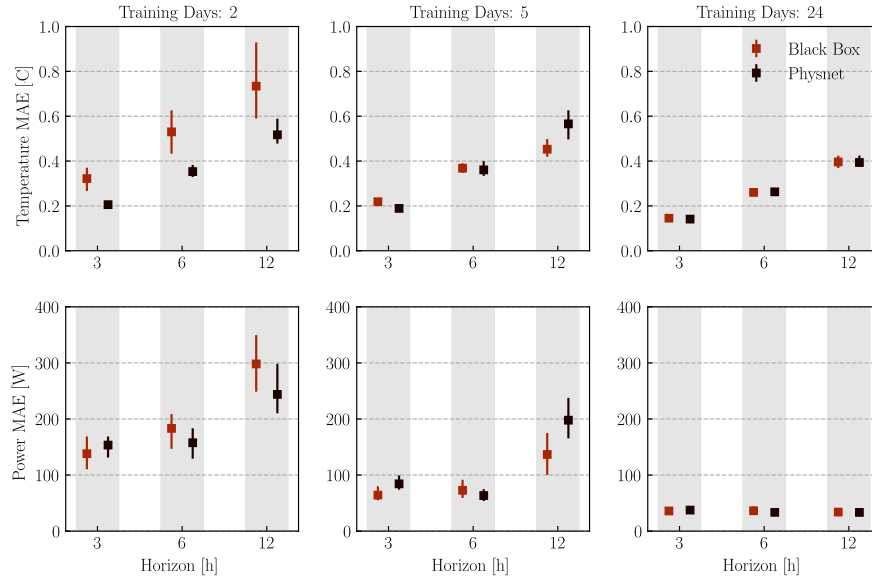


Figure 4: Prediction results of the PhysNet architecture and its Black-Box counterpart with different training sizes and prediction horizons.

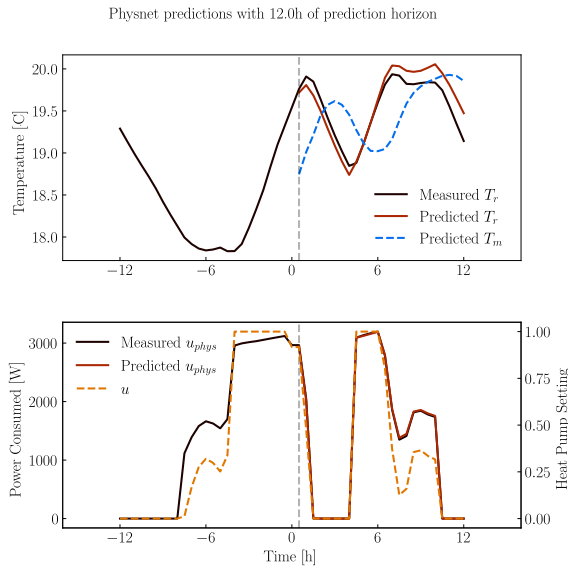


Figure 5: PiNN predictions with a horizon of 12 hours.

MCTS algorithm compared to its Vanilla version, especially when a low number of tree traversals is used. Note that for real-world applications there needs to be a balance between performance and computational effort required. The results presented in Fig. 8 demonstrate that the AlphaZero MCTS controller can efficiently find valid control actions with a lower number of simulations, leading to a controller that can be (potentially) deployed in real-world buildings in a scalable manner.

6. Conclusions

In this paper, we presented an MCTS algorithm with a PiNN applied to a residential heating Demand Response problem. We showed the control benefits of the PiNN simulator compared to a Black-Box one. We then used a Deep Learning infused MCTS algorithm inspired by AlphaZero to evaluate its efficiency benefits compared to a more standard version, showing promising results for the AlphaZero-based technique. Thanks to its flexibility to incorporate state-dependent constraints on the allowed actions, we believe MCTS can be a valid technique for Demand Response control of a residential heater. The results show that MCTS control performance is remarkable, especially when a physically infused model is used.

Following this work, different research directions can be made to further explore MCTS in this scope. To list a few that we consider the most relevant: a complete comparison between the MCTS techniques and state-of-the-art control algorithms would further clarify the potential of these methods. Further refining of the MCTS algorithm based on recent evolutions in that field (e.g., MuZero [5]) is a direction of future work. Also, in settings where the constraints considered vary dynamically over time, MCTS could be even more beneficial. Future works will explore this aspect in more details. Finally, while this paper established the potential of advanced MCTS techniques for heat pump control, further validation in real-world deployments should be carried out.

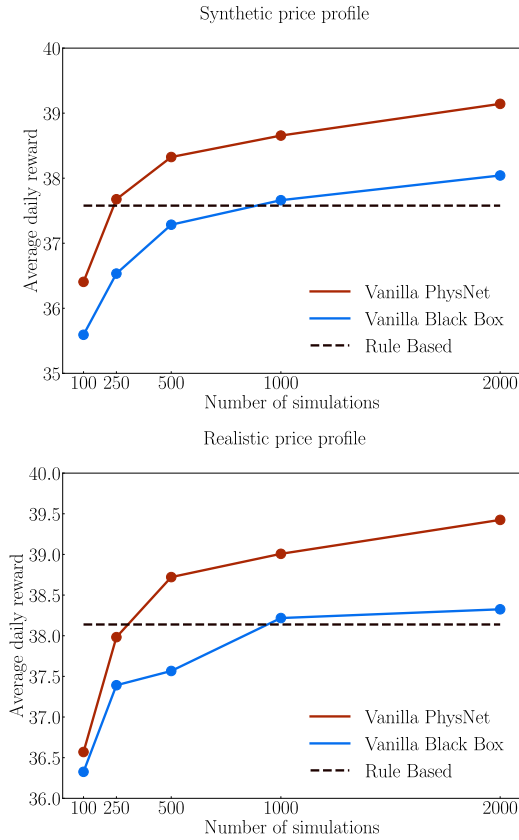


Figure 6: Average daily rewards obtained by the Vanilla MCTS when applied to 11 test days with a PhysNet and a Black-Box simulator.

Declaration of Competing Interest

The authors declare that they have no known competing financial interests or personal relationships that could have appeared to influence the work reported in this paper.

Acknowledgments and funding

This work was supported by the European Union’s Horizon 2020 research and innovation programme under the projects BRIGHT (grant agreement no. 957816) and BIGG (grant agreement no. 957047).

We also thank Marie-Sophie Verwee for her technical support in the deployment of our work.

A. Hyperparameters

The PhysNet network is composed of two separate Feed Forward Neural Networks (FFNNs), the encoder and the predictor. The encoder has a single hidden layer composed of 32 neurons activated with a ReLU function. Its output layer is activated with a tanh function. The predictor has a single hidden layer composed of 64 neurons activated with a ReLU function. The output of the predictor layer has two different activation functions: tanh for the temperature, and ReLU for the energy consumption. The past observations depth value

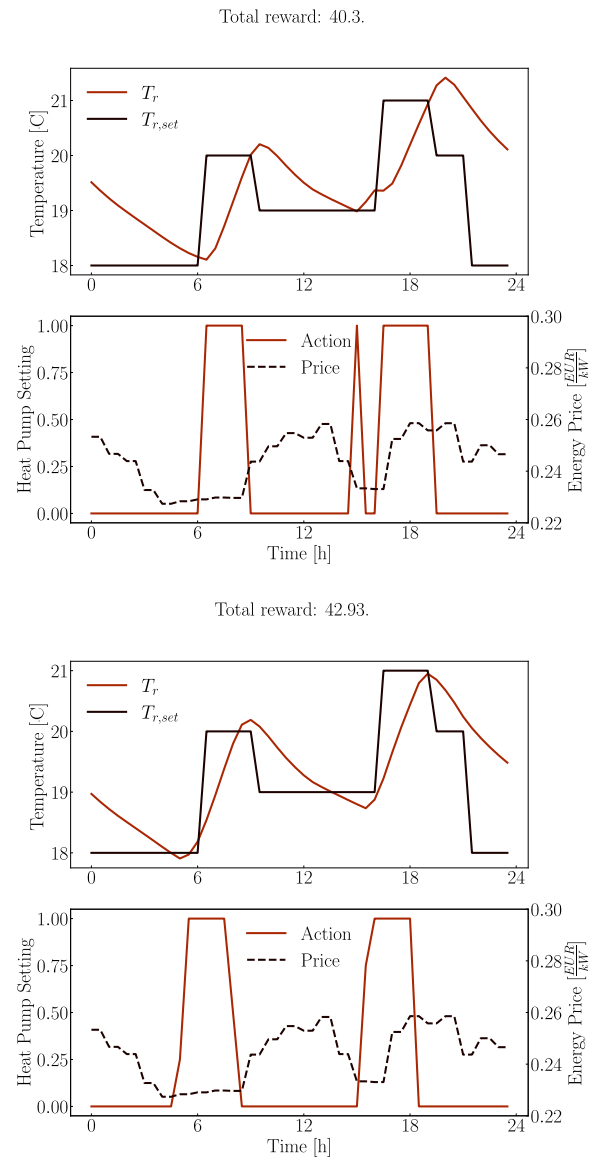


Figure 7: Action sequence selected by the rule-based bang-bang policy and the PhysNet-based Vanilla MCTS respectively. The two policies are considered in the same days. The MCTS policy is able to remain closer to the desired temperature while heating the room at lower price slots; resulting in a higher reward compared to the rule-based controller.

d is fixed to 24 time-steps (12 hours). All the neural network parameters are trained with an Adam optimizer. The prior policy neural network $p(\tilde{x})$ of the AlphaZero algorithm is a FFNN with 2 hidden layers of 64 and 32 neurons activated with a ReLU function. Its final output gets activated through a softmax function and the whole network gets trained with a Cross-Entropy loss and an Adam optimizer. All the neural networks used in this paper were implemented using PyTorch 2.0 [54].

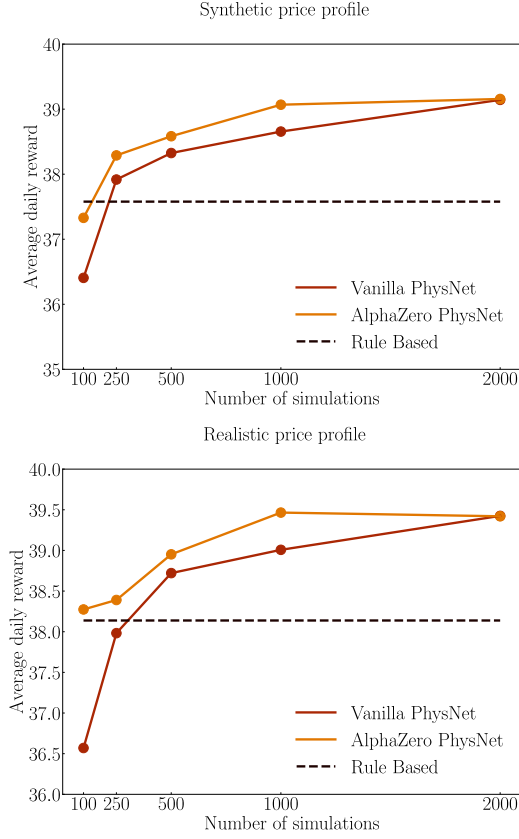


Figure 8: Average daily rewards obtained by the Vanilla MCTS and AlphaZero MCTS when applied to 11 test days with a PhysNet simulator.

B. Rule Based Controllers

The rule-based bang-bang controller referred to in this work heats the room whenever its temperature drops below the desired one. Mathematically, its policy is defined as:

$$u_t = \begin{cases} 1 & \text{if } T_{r,t} < T_{r,set,t} \\ 0 & \text{otherwise} \end{cases} \quad (11)$$

The discrete rule-based controller is defined as:

$$u_t = \begin{cases} 0 & \text{if } T_{r,t} > T_{r,set,t} \\ 0.25 & \text{else if } T_{r,t} > T_{r,set,t} - 0.05 \\ 0.5 & \text{else if } T_{r,t} > T_{r,set,t} - 0.15 \\ 0.75 & \text{else if } T_{r,t} > T_{r,set,t} - 0.25 \\ 1 & \text{otherwise} \end{cases} \quad (12)$$

Finally, the continuous controller used to generate data in Section 5.1 is defined as:

$$u_t = \min(2(T_{r,set,t} - T_{r,t})^+, 1) \quad (13)$$

C. Cumulative noise

To evaluate our experiments in a more realistic manner, we added random noise to the future outside temperature

used in the forecast and in the control problems. For each time-step, we randomly chose a binary value to determine the sign of the added noise (positive or negative). We then sampled and added random noise from a normal distribution to the outside temperature. The noise added gets cumulated while considering values more far into the future. Each addition get multiplied with a σ (or $-\sigma$) hyperparameter that determines the magnitude of the added noise

CRedit authorship contribution statement

Fabio Pavirani: Conceptualization, Methodology, Software, Formal analysis, Investigation, Visualization, Writing - Original Draft. **Gargya Gokhale:** Software, Conceptualization, Writing - Review & Editing. **Bert Claessens:** Supervision, Conceptualization, Writing - Review & Editing. **Chris Develder:** Supervision, Funding acquisition, Writing - Review & Editing.

References

- [1] Eurostat, 2020. Energy, transport and environment statistics — 2020 edition.
- [2] Stoffel, P., Maier, L., Kümpel, A., Schreiber, T., Müller, D., 2023. Evaluation of advanced control strategies for building energy systems. *Energy and Buildings* 280, 112709.
- [3] Wang, Z., Hong, T., 2020. Reinforcement learning for building controls: The opportunities and challenges. *Applied Energy* 269, 115036.
- [4] Nagy, Z., Henze, G., Dey, S., Arroyo, J., Helsen, L., Zhang, X., Chen, B., Amasyali, K., Kurte, K., Zamzam, A., et al., 2023. Ten questions concerning reinforcement learning for building energy management. *Building and Environment*, 110435.
- [5] Schrittwieser, J., Antonoglou, I., Hubert, T., Simonyan, K., Sifre, L., Schmitt, S., Guez, A., Lockhart, E., Hassabis, D., Graepel, T., et al., 2020. Mastering atari, go, chess and shogi by planning with a learned model. *Nature* 588, 604–609.
- [6] Gokhale, G., Claessens, B., Develder, C., 2022. Physics informed neural networks for control oriented thermal modeling of buildings. *Applied Energy* 314, 118852.
- [7] Boodi, A., Beddiar, K., Benamour, M., Amirat, Y., Benbouzid, M., 2018. Intelligent systems for building energy and occupant comfort optimization: A state of the art review and recommendations. *Energies* 11, 2604.
- [8] Afroz, Z., Shafiullah, G., Urmee, T., Higgins, G., 2018. Modeling techniques used in building hvac control systems: A review. *Renewable and sustainable energy reviews* 83, 64–84.
- [9] Homod, R.Z., 2013. Review on the hvac system modeling types and the shortcomings of their application. *Journal of Energy* 2013.
- [10] Fouquier, A., Robert, S., Suard, F., Stéphan, L., Jay, A., 2013. State of the art in building modelling and energy performances prediction: A review. *Renewable and Sustainable Energy Reviews* 23, 272–288.
- [11] Li, X., Wen, J., 2014. Review of building energy modeling for control and operation. *Renewable and Sustainable Energy Reviews* 37, 517–537.
- [12] Deb, C., Zhang, F., Yang, J., Lee, S.E., Shah, K.W., 2017. A review on time series forecasting techniques for building energy consumption. *Renewable and Sustainable Energy Reviews* 74, 902–924.
- [13] Bourdeau, M., qiang Zhai, X., Nefzaoui, E., Guo, X., Chatellier, P., 2019. Modeling and forecasting building energy consumption: A review of data-driven techniques. *Sustainable Cities and Society* 48, 101533.
- [14] Ali, U., Shamsi, M.H., Hoare, C., Mangina, E., O'Donnell, J., 2021. Review of urban building energy modeling (ubem) approaches, methods and tools using qualitative and quantitative analysis. *Energy and*

- buildings 246, 111073.
- [15] Wetter, M., Zuo, W., Nouidui, T.S., Pang, X., 2014. Modelica buildings library. *Journal of Building Performance Simulation* 7, 253–270.
- [16] Crawley, D.B., Lawrie, L.K., Winkelmann, F.C., Buhl, W.F., Huang, Y.J., Pedersen, C.O., Strand, R.K., Liesen, R.J., Fisher, D.E., Witte, M.J., et al., 2001. Energyplus: creating a new-generation building energy simulation program. *Energy and buildings* 33, 319–331.
- [17] Szegedy, C., Zaremba, W., Sutskever, I., Bruna, J., Erhan, D., Goodfellow, I., Fergus, R., 2013. Intriguing properties of neural networks. arXiv preprint arXiv:1312.6199 .
- [18] Di Natale, L., Svetozarevic, B., Heer, P., Jones, C.N., 2022. Physically consistent neural networks for building thermal modeling: theory and analysis. *Applied Energy* 325, 119806.
- [19] Afram, A., Janabi-Sharifi, F., 2015. Gray-box modeling and validation of residential hvac system for control system design. *Applied Energy* 137, 134–150.
- [20] Matthijs, B., Azzam, A., Binder, J., 2023. Thermal building models for energy management systems, in: 2023 IEEE International Conference on Environment and Electrical Engineering and 2023 IEEE Industrial and Commercial Power Systems Europe (EEEIC/I&CPS Europe), IEEE. pp. 1–6.
- [21] Bacher, P., Madsen, H., 2011. Identifying suitable models for the heat dynamics of buildings. *Energy and buildings* 43, 1511–1522.
- [22] Vrettos, E., Kara, E.C., MacDonald, J., Andersson, G., Callaway, D.S., 2016. Experimental demonstration of frequency regulation by commercial buildings—part i: Modeling and hierarchical control design. *IEEE Transactions on Smart Grid* 9, 3213–3223.
- [23] Raissi, M., Perdikaris, P., Karniadakis, G.E., 2019. Physics-informed neural networks: A deep learning framework for solving forward and inverse problems involving nonlinear partial differential equations. *Journal of Computational physics* 378, 686–707.
- [24] Hochreiter, S., Schmidhuber, J., 1997. Long short-term memory. *Neural computation* 9, 1735–1780.
- [25] LeCun, Y., Bottou, L., Bengio, Y., Haffner, P., 1998. Gradient-based learning applied to document recognition. *Proceedings of the IEEE* 86, 2278–2324.
- [26] Schroff, F., Kalenichenko, D., Philbin, J., 2015. Facenet: A unified embedding for face recognition and clustering, in: *Proceedings of the IEEE conference on computer vision and pattern recognition*, pp. 815–823.
- [27] Drgoña, J., Tuor, A.R., Chandan, V., Vrabie, D.L., 2021. Physics-constrained deep learning of multi-zone building thermal dynamics. *Energy and Buildings* 243, 110992.
- [28] Drgoña, J., Arroyo, J., Figueroa, I.C., Blum, D., Arendt, K., Kim, D., Ollé, E.P., Oravec, J., Wetter, M., Vrabie, D.L., et al., 2020. All you need to know about model predictive control for buildings. *Annual Reviews in Control* 50, 190–232.
- [29] Yao, Y., Shekhar, D.K., 2021. State of the art review on model predictive control (mpc) in heating ventilation and air-conditioning (hvac) field. *Building and Environment* 200, 107952.
- [30] Afram, A., Janabi-Sharifi, F., Fung, A.S., Raahemifar, K., 2017. Artificial neural network (ann) based model predictive control (mpc) and optimization of hvac systems: A state of the art review and case study of a residential hvac system. *Energy and Buildings* 141, 96–113.
- [31] Lee, Y.M., Horesh, R., Liberté, L., 2015. Optimal hvac control as demand response with on-site energy storage and generation system. *Energy Procedia* 78, 2106–2111.
- [32] Reynolds, J., Rezgui, Y., Kwan, A., Piriou, S., 2018. A zone-level, building energy optimisation combining an artificial neural network, a genetic algorithm, and model predictive control. *Energy* 151, 729–739.
- [33] Chen, J., Augenbroe, G., Song, X., 2018. Lighted-weighted model predictive control for hybrid ventilation operation based on clusters of neural network models. *Automation in Construction* 89, 250–265.
- [34] Ławryńczuk, M., 2014. Computationally efficient model predictive control algorithms. A Neural Network Approach, *Studies in Systems, Decision and Control* 3.
- [35] Brandi, S., Piscitelli, M.S., Martellacci, M., Capozzoli, A., 2020. Deep reinforcement learning to optimise indoor temperature control and heating energy consumption in buildings. *Energy and Buildings* 224, 110225.
- [36] Wei, T., Wang, Y., Zhu, Q., 2017. Deep reinforcement learning for building hvac control, in: *Proceedings of the 54th annual design automation conference 2017*, pp. 1–6.
- [37] Patyn, C., Ruelens, F., Deconinck, G., 2018. Comparing neural architectures for demand response through model-free reinforcement learning for heat pump control, in: 2018 IEEE international energy conference (ENERGYCON), IEEE. pp. 1–6.
- [38] Nagy, A., Kazmi, H., Cheaib, F., Driesen, J., 2018. Deep reinforcement learning for optimal control of space heating. arXiv preprint arXiv:1805.03777 .
- [39] Jiang, Z., Risbeck, M.J., Ramamurti, V., Murugesan, S., Amores, J., Zhang, C., Lee, Y.M., Drees, K.H., 2021. Building hvac control with reinforcement learning for reduction of energy cost and demand charge. *Energy and Buildings* 239, 110833.
- [40] Wijaya, T.K., Papaioannou, T.G., Liu, X., Aberer, K., 2013. Effective consumption scheduling for demand-side management in the smart grid using non-uniform participation rate, in: 2013 Sustainable Internet and ICT for Sustainability (SustainIT), IEEE. pp. 1–8.
- [41] Galván-López, E., Harris, C., Trujillo, L., Rodríguez-Vazquez, K., Clarke, S., Cahill, V., 2014. Autonomous demand-side management system based on monte carlo tree search, in: 2014 IEEE International Energy Conference (ENERGYCON), IEEE. pp. 1263–1270.
- [42] Golpayegani, F., Dusparic, I., Clarke, S., 2015. Collaborative, parallel monte carlo tree search for autonomous electricity demand management, in: 2015 Sustainable Internet and ICT for Sustainability (SustainIT), IEEE. pp. 1–8.
- [43] Golpayegani, F., Dusparic, I., Taylor, A., Clarke, S., 2016. Multi-agent collaboration for conflict management in residential demand response. *Computer Communications* 96, 63–72.
- [44] Kiljander, J., Sarala, R., Rehu, J., Pakkala, D., Pääkkönen, P., Takalo-Mattila, J., Känslä, K., 2021. Intelligent consumer flexibility management with neural network-based planning and control. *IEEE Access* 9, 40755–40767.
- [45] Silver, D., Schrittwieser, J., Simonyan, K., Antonoglou, I., Huang, A., Guez, A., Hubert, T., Baker, L., Lai, M., Bolton, A., et al., 2017. Mastering the game of go without human knowledge. *nature* 550, 354–359.
- [46] Silver, D., Hubert, T., Schrittwieser, J., Antonoglou, I., Lai, M., Guez, A., Lanctot, M., Sifre, L., Kumaran, D., Graepel, T., et al., 2018. A general reinforcement learning algorithm that masters chess, shogi, and go through self-play. *Science* 362, 1140–1144.
- [47] Busoniu, L., Babuska, R., De Schutter, B., Ernst, D., 2017. Reinforcement learning and dynamic programming using function approximators. CRC press.
- [48] Coulom, R., 2006. Efficient selectivity and backup operators in monte-carlo tree search, in: *International conference on computers and games*, Springer. pp. 72–83.
- [49] Kocsis, L., Szepesvári, C., 2006. Bandit based monte-carlo planning, in: *European conference on machine learning*, Springer. pp. 282–293.
- [50] Rosin, C.D., 2011. Multi-armed bandits with episode context. *Annals of Mathematics and Artificial Intelligence* 61, 203–230.
- [51] Silver, D., Huang, A., Maddison, C.J., Guez, A., Sifre, L., Van Den Driessche, G., Schrittwieser, J., Antonoglou, I., Panneershelvam, V., Lanctot, M., et al., 2016. Mastering the game of go with deep neural networks and tree search. *nature* 529, 484–489.
- [52] Blum, D., Arroyo, J., Huang, S., Drgoña, J., Jorissen, F., Walnum, H.T., Chen, Y., Benne, K., Vrabie, D., Wetter, M., et al., 2021. Building optimization testing framework (boptest) for simulation-based benchmarking of control strategies in buildings. *Journal of Building Performance Simulation* 14, 586–610.
- [53] Arroyo, J., Manna, C., Spiessens, F., Helsen, L., 2021. An open-ai gym environment for the building optimization testing (boptest) framework, in: *Building Simulation 2021, IBPSA*. pp. 175–182.

- [54] Paszke, A., Gross, S., Massa, F., Lerer, A., Bradbury, J., Chanan, G., Killeen, T., Lin, Z., Gimelshein, N., Antiga, L., Desmaison, A., Kopf, A., Yang, E., DeVito, Z., Raison, M., Tejani, A., Chilamkurthy, S., Steiner, B., Fang, L., Bai, J., Chintala, S., 2019. Pytorch: An imperative style, high-performance deep learning library, in: Advances in Neural Information Processing Systems 32. Curran Associates, Inc., pp. 8024–8035.